American Mineralogist, Volume 87, pages 609–622, 2002

High-pressure IR-spectra and the thermodynamic properties of chloritoid

MONIKA KOCH-MÜLLER,[1,2,*] ANNE M. HOFMEISTER,[3] YINGWEI FEI,[1] AND ZHENXIAN LIU[1]

[1]Geophysical Laboratory, Center of High Pressure Research, Carnegie Institution of Washington, 5251 Broad Branch Road N.W., Washington, D.C. 20015, U.S.A.
[2]GeoForschungsZentrum Potsdam, Projektbereich 4.1, Telegrafenberg, 14473 Potsdam, Germany
[3]Department of Earth and Planetary Science, Washington University, Box 1169, 1 Brookings Drive, St. Louis, Missouri 63130, U.S.A.

ABSTRACT

Using IR radiation from a synchrotron source, high-quality absorbance spectra were obtained from polycrystalline powder of chloritoid (cld) from ambient conditions up to pressures of 10 GPa over 50 to 4000 cm^{-1}. The idealized chemical composition of the chloritoid group is $M_2Al_4O_2(SiO_4)_2(OH)_4$ where M = Fe or Mg in our experiments. All of the 42 expected fundamental IR modes were observed. These data, combined with the response of the IR bands to substitutions of Fe for Mg, and of D for H, constrained the band assignments. Heat capacity (C_P) and entropy (S_o) for the triclinic and monoclinic polymorphs of Fe- and Mg-cld were calculated from the Kieffer-type model, using our detailed band assignments. The calculated heat capacity and entropy for the monoclinic and triclinic polymorphs differ negligibly. The results at temperatures above 298 K are described by the following polynomial expressions in J/(mol·K): $C_P = 7.835 \cdot 10^2 - 5.170 \cdot 10^3 T^{-0.5} - 1.648 \cdot 10^7 T^{-2} + 1.934 \cdot 10^9 T^{-3}$ for Mg-cld and $C_P = 7.848 \cdot 10^2 - 5.185 \cdot 10^3 T^{-0.5} - 1.548 \cdot 10^7 T^{-2} + 1.783 \cdot 10^9 T^{-3}$ for Fe-cld. At room temperature, $S_o = 293$ J/mol·K for Mg-cld and 335 J/mol·K for Fe-cld. These values differ somewhat from entropy estimated from various internally consistent databases (–3 to –9% for Mg-cld and –9 to +5% for Fe-cld). However, using our new S_o and C_P values in conjunction with the enthalpy of formation, $H_f = -7101$ kJ/mol for Mg-cld or $H_f = -6422$ kJ/mol for Fe-cld (estimated in this study), we can closely reproduce the experimental data for the reactions Mg-chloritoid + talc = clinochlore + kyanite (Chopin 1985) and Fe-chloritoid = almandine + diaspore + water (Vidal et al. 1994).

INTRODUCTION

Chloritoid is a characteristic mineral of Al-rich, low-temperature metapelitic rocks. This orthosilicate has the general formula $(Fe,Mg)_2(Al, Fe^{3+})Al_3$ $[(SiO_4)_2O_2(OH)_4]$. Fe-rich chloritoid is characteristically found in rocks of low metamorphic grade, whereas magnesiochloritoid is a key mineral in high-pressure pelitic blueschists (e.g., Chopin 1983; Chopin and Monié 1984; Simon et al. 1997; Messiga et al. 1999). Due to their restricted occurrences, Fe- and Mg-chloritoid are important geobarometric and geothermometric markers. The stability of Fe-chloritoid has been investigated by Ganguly (1969), Rao and Johannes (1979), and Vidal et al. (1994), whereas the stability of Mg-chloritoid was examined by Chopin (1985). These experimental data were used in internally consistent databases to derive thermodynamic parameters for chloritoid (Gottschalk 1997; Chatterjee et al. 1998; Holland and Powell 1998). However, the results are not entirely consistent. For example, the entropy ranges from 303 (Chatterjee et al. 1998) to 352 J/(mol·K) (Helgeson et al. 1978) for Fe-chloritoid and from 264 (Holland and Powell 1998) to 284 J/(mol·K) (Vidal et al. 1999) for Mg-chloritoid. To date, the thermodynamic properties of chloritoid have not been measured directly.

Thermodynamic data such as heat capacity and entropy can be calculated from vibrational spectroscopy (Kieffer 1979, 1980). In this approach, the measured IR and/or Raman spectra are used to construct a model for the density of states. The advantage of this method is that only a small sample amount is needed. If the spectra are collected from powders, then the model usually reproduces heat capacities C_P to within 5% at 298 K and 1% at 700 K (Cynn et al. 1996). Complete IR spectra and accurate band assignments improves the accuracy to ~0.5% (Hofmeister and Chopelas 1991). Infrared spectra of natural, monoclinic, and triclinic chloritoid have been reported by Moenke (1962), Fransolet (1978), and De Grave et al. (1984) from ~400–4000 cm^{-1}. Chopin et al. (1992) obtained IR spectra of synthetic magnesiochloritoid from 200 to 4000 cm^{-1}. However, IR bands could exist at lower frequency, and these can strongly influence the calculations.

This paper presents the first far- to near-IR spectra of triclinic (Fe,Mg)-chloritoids at ambient condition and as a function of pressure. We utilized synchrotron IR radiation to obtain an excellent signal-to-noise ratio, which is crucial for the in situ measurements at high pressure. All 42 IR active modes were observed and assigned to atomic motions based on these data and supplementary information from chemical substitutions. With these assignments we constructed the density of

* E-mail: mkoch@gfz-potsdam.de

state and calculated the entropy and heat capacity data for chloritoids.

STRUCTURE

Chloritoid occurs in at least two modifications: a triclinic form (space group $C\bar{1}$) and a monoclinic form (space group $C2/c$). The crystal structure of natural, monoclinic chloritoid was investigated by Brindley and Harrison (1952), Harrison and Brindley (1957), Hanscom (1975), Ivaldi et al. (1988), and Comodi et al. (1992). Hanscom (1980) studied natural triclinic chloritoid. The structure contains alternating layers of edge-connected octahedra, oriented perpendicular to **c**. Layer L1 is composed of edge sharing M1A octahedra that contain Al or Fe^{3+} and of M1B octahedra with Fe^{2+} or Mg. Layer L2 consists of edge-sharing M2A and M2B octahedra, both of which contain Al. The two layers L1 and L2 are linked by isolated Si tetrahedra (T) and by the hydrogen atoms H1A and H1B. The structure of the triclinic polymorph resembles the monoclinic structure, but has one layer of each type L1 and L2 in the triclinic unit cell, rather than two of each, as in the monoclinic unit cell. The reduction of the symmetry from monoclinic to triclinic is mainly caused by displacements in the L2 layer: the M2B site is located on two special positions in the triclinic structure, whereas it occupies a general position in the monoclinic form.

Comodi et al. (1992) investigated the effect of the pressure on the crystal structure of natural, monoclinic Mg-rich chloritoid up to 4.2 GPa by in situ single-crystal X-ray diffraction in a diamond anvil cell. They obtained a very high bulk modulus of 148 Gpa, which is unusual for a layered mineral but resembles values for close-packed structures such as forsterite with Ks = 131 GPa (Zha et al. 1998). The bulk moduli for the different polyhedra increase from 53 and 63 GPa for the M1A and M1B polyhedra to 116 and 144 GPa for the Al2B and Al2A octahedra. They found that the SiO_4 tetrahedra are incompressible in the investigated pressure range. Thus, the polyhedra have quite different structural properties and respond to substitutions (Fe-Mg) and changes in pressure in a quite distinct way. These changes must be reflected in the IR spectra and will be useful to assign the IR bands.

SYMMETRY ANALYSIS

Triclinic $Mg_2Al_4Si_2O_{10}(OH)_4$ with $Z = 1$ for the non-centered primitive unit cell should have 78 vibrational modes, whereas monoclinic chloritoid with $Z = 2$ for the non-centered primitive unit cell should have 156 modes. Factor group analysis (Farmer and Lazarev 1974) was used to classify the number, type, and symmetry of these vibrational modes (Table 1). Three modes are acoustic: all of the remaining modes are either IR or Raman active.

As a first approximation, the internal modes of the isolated SiO_4 tetrahedra are treated as preserved entities, leading to 18 modes for triclinic and 36 modes for monoclinic chloritoid (Table 1). Only the O2A, O2B, O2C, and O1C oxygen atoms are involved in the internal SiO_4 motions. The remaining O atoms produce additional vibrational modes. For example, bonding of O1A and O1B to M1B and of O2D to M2B yield stretching motions (Table 1). The symmetry analysis was com-

TABLE 1. Classification of normal modes of monoclinic and triclinic chloritoid by the correlation method and site group analysis

			Monoclinic				Triclinic	
Atom	Site Symmetry ‡	No§	A_g*	B_g*	A_u†	B_u†	A_g*	A_u†
Si	C_1 m, t	4 (2)	3	3	3	3	3	3
M1B (Mg, Fe)	C_1 m, t	4 (2)	3	3	3	3	3	3
M2B m; M2B1 t (Al)	C_1 m, C_1 t	4 (1)	3	3	3	3	0	3
M2B2 (Al)	– m, C_1 t	– (1)	–	–	–	–	0	3
M1A (Al)	C_1 m, t	2 (1)	0	0	3	3	0	3
M2A (Al)	C_2 m, C_1 t	2 (1)	1	2	1	2	0	3
O1A, O1B, O1C, O2A, O2B, O2C, O2D	C_1 m, t	28 (14)	21	21	21	21	21	21
H1A, H1B	C_1 m, t	8 (4)	6	6	6	6	6	6
Total			37	38	40	41	33	45
Acoustic					1	2		3
Optic			37	38	39	39	33	42
			Factor group analysis					
Si-O sym. stretching ν_1			1	1	1	1	1	1
O-Si-O sym. bending ν_2			2	2	2	2	2	2
Si-O asym. stretching ν_3			3	3	3	3	3	3
O-Si-O asym. bending ν_4			3	3	3	3	3	3
R (Si)			3	3	3	3	3	3
T (Si)			3	3	3	3	3	3
T (M1A)			0	0	3	3	0	3
T (M1B)			3	3	3	3	3	3
T (M2A)			1	2	0 ‖	0 ‖	0	0 ‖
T (M2B) no.			3	3	3	3	0	6
O-M1B-O stretching			3	3	3	3	3	3
O-M1B-O bending			3	3	3	3	3	3
M2B-O2D stretching			3	3	3	3	3	3
O1A-H1A 1 stretching; 2 bending			3	3	3	3	3	3
O1B-H1B 1 stretching; 2 bending			3	3	3	3	3	3

* Raman active.
† IR active.
‡ m for monoclinic, t for triclinic.
§ Number of atoms in the primitive monoclinic (triclinic) cell.
‖ Acoustic modes are subtracted.
In triclinic cld the M2B site is located on two special positions M2B1 and M2B2.

pleted by allocating the remaining vibrations to translation of the M cations (Table 1).

EXPERIMENTAL METHODS

Synthesis and sample characterization

Fe- and Mg-chloritoids of different compositions were synthesized at the Technische Universität Berlin in a piston-cylinder apparatus using rock-salt cells at 2.0–2.5 GPa and about 600 °C and at the Bayerische Geoinstitut Bayreuth at 3.5 GPa in piston-cylinder devices using oxide mixtures and water in excess. Powder X-ray diffraction data revealed that chloritoid crystallizes in the triclinic space group $C\bar{1}$ and that the Fe-Mg chloritoid solid solution exhibits no excess volume. According to the Mössbauer spectra of the Fe-Mg chloritoids, the Fe^{3+} content is very low (1–4 wt% of the total Fe content). The compositions and crystal chemistry of the chloritoid samples studied here are given in Koch-Müller et al. (2000a) and Koch-Müller and Wirth (2001). One additional sample (MKM-98-34; $x_{Fe} = 0.74$) was synthesized with D_2O instead of water.

Some synthesized products involving Mg-rich chloritoids contain staurolite, quartz, and/or corundum as additional phases. The relatively coarse-grained quartz and corundum crystals could be removed from the starting material by hand picking under a stereomicroscope. To obtain pure samples of Mg-rich chloritoid, we isolated the lighter magnesiochloritoid ($\rho \approx 3.17$ g/cm^3) from the heavier staurolite ($\rho \approx 3.5$ g/cm^3) by heavy liquid gravity separation using methyleniodid ($\rho = 3.3$ g/cm^3). X-ray diffraction and IR spectroscopy revealed that the recovered lighter fraction is nearly 100% pure chloritoid.

Infrared spectroscopy

For the near- to mid-IR measurements at ambient conditions, 1.3 mg of the ground synthetic chloritoid powders were mixed with 450 mg KBr and pressed to disks of 13 mm diameter under vacuum. The chloritoid powders and the KBr were dried at 120 °C before and after mixing to eliminate adsorbed water. Measurements were made on a Bruker IFS66v FTIR spectrometer equipped with a Globar light source, a KBr beamsplitter, and a DTGS detector at the GeoForschungsZentrum Potsdam. The spectra of eight synthetic, triclinic Fe-Mg chloritoid solid solutions and of the triclinic Fe- and Mg-end-members were collected. The operating conditions for the spectrometer were 2 cm^{-1} resolution and 254 averaged scans.

In situ high-pressure mid- and far-IR spectra were obtained with a Bruker ISF 66v FTIR spectrometer at the U2A beamline at the National Synchrotron Light Source, Brookhaven National Laboratory. The spectrometer was equipped with a modified IRscopeII mid-IR microscope and a custom-designed microscope system for far-IR measurements. For mid-IR measurements, we used a Megabar-type diamond-anvil cell (Mao and Hemley 1998) with type II diamonds and a stainless steel gasket. Thin films of Fe- and Mg-chloritoid end-members of micrometer-size thicknesses were created for these measurements by pressing the corresponding powdered chloritoid samples in a diamond anvil cell without gasket. The films were then embedded in the gasket hole (diameter of 100 µm) with ruby grains for the pressure measurements and NaCl as a pressure medium. The aperture was set to 20×30 µm^2 and the spectra were acquired in the range of 600–8000 cm^{-1} with a KBr beamsplitter and an MCT detector. A resolution of 4 cm^{-1} from 1024 scans was used for every spectrum. The pressure was determined from the energy shift of the R_1 ruby fluorescence line relative to its energy at ambient conditions (Mao et al. 1986).

For far-IR measurements, the spectra were collected from 50–400 cm^{-1} with a Mylar beamsplitter and a helium cooled bolometer. The entire optical path was purged with dry N_2 during the measurements to eliminate vapor absorption. For measurements at high pressure we used a Megabar-type diamond-anvil cell (Mao and Hemley 1998) with type I diamonds with culet sizes between 750 and 850 µm. For the ambient spectra, chloritoid powder was put without pressure medium on one anvil diamond and the cell was carefully closed without pressurizing. The estimated sample thickness was about 40 µm. This thickness was needed to enhance the weak far-IR absorption bands but it prevents measurement of the intense peaks at wavenumbers >400 cm^{-1} which were off-scale. The spectra were collected from six synthetic triclinic Fe-Mg solid solutions, the triclinic Fe- and Mg-end-members, and a monoclinic natural chloritoid sample. For the high-pressure measurements 30 µm thick disks of triclinic Fe- and Mg-chloritoid end-members and of a natural triclinic Fe-Mg solid solution were created by compressing the powdered samples in an ungasketed diamond anvil cell. Then a pre-indented stainless steel gasket with a 400 µm hole was mounted on top of one diamond anvil. The samples were embedded in the gasket hole with ruby grains for pressure calibration and petroleum jelly as a pressure medium. The spectra were recorded with a resolution of 4 cm^{-1} from 512 scans and no aperture was used during the measurements.

Raman spectroscopy

Raman spectra were recorded with a multichannel Raman microprobe (Dilor XY) in a backscattering configuration using a CCD detector with 1024×298 channels. The excitation source was an Argon-Ion laser operated at 514.5 nm to compensate for the green color of the chloritoid crystals. The laser light was focused onto the sample using a Leitz L25 objective. Typical acquisition time was 10–15 min. The sample consists of single crystals of a natural triclinic chloritoid sample. Because the intensity of the modes varies with the orientation of the single crystal, several spectra with different orientations for one single crystal were collected in order to isolate certain Raman active modes and an average in the peak position was taken for each band.

RESULTS

IR Spectroscopy

The IR frequencies for triclinic chloritoids are listed in Tables 2 and 3. Our spectra are in good agreement with those from previous studies (most recently, De Grave et al. 1984; Chopin et al. 1992; Koch-Müller et al. 2000b). Three additional bands were detected in the frequency range examined previously, and new data were obtained below 200 cm^{-1}. We also listed band assignments made on the basis of the changes in frequency upon compression or chemical substitution (Table 2

TABLE 2. Near- and mid-IR bands and Mode Grüneisen parameters for triclinic Fe- and Mg-cld

	IR Fe-cld (MKM-97-8)			IR Mg-cld (MKM-98-43)			Mode	Raman
No	ν_{i0} (cm^{-1})	$\delta\nu/\delta P$ (cm^{-1}/GPa)	γ_{i0} *	ν_{i0} (cm^{-1})	$\delta\nu/\delta P$ (cm^{-1}/GPa)	γ_{i0} *		x_{Fe} = 0.59
1	3463.0	4.448	0.20	3490.8	5.050	0.21	O-HB	3455
2	2989.3	–11.640	–0.59	3056.6	–11.104	–0.53	O-HA	3076
OT	2162.0	4.311	0.30	2159.8	5.140	0.35	2× mode 3	
3	1103.4	2.453	0.34	1093.5	3.636	0.49	δO-H1A †	1096
4				1035.7	3.176	0.45	ν_3	
5	973.4	3.394	0.53	986.5	5.592	0.84	O-M1B-O	985
6, 7	953.1			966.1	5.578	0.85	O-M1B-O, γO-H1A ‡	909
8				930.9	5.087	0.81	O-M1B-O	
9	898.5	3.458	0.58	906.7	3.613	0.59	ν_1	881
10	851.6	–0.939	–0.15	867.8	2.146	0.37	γO-H1B ‡	847
11	810.3			823.2	3.711	0.67	ν_3	805
12	743.9	1.805	0.37	758.2	3.977	0.78	ν_3.	738
13	726.7			740.6	4.240	0.85	δO-H1B †	
14	679.4	2.000	0.45	692.3	4.289	0.92	O-M1B-O	
15	665.1	0.824	0.19	672.9	0.941	0.21	M2B-O	
16				639.9	3.495	0.81	M2B-O	
17	609.4	2.187	0.55	614.9	3.750	0.90	M2B-O	
18	586.4	1.526	0.40	596.5	2.633	0.65	ν_2+ν_4	594
19	561.1			576.3			O-M1B-O	
20	547.5			550.3			ν_2+ν_4	551
21	511.6			518.8			ν_2+ν_4	531
22	483.2			485.4			ν_2+ν_4	513
23	452.3			462.5			ν_2+ν_4	412
24	440.8			453.3			T (M1A)	
25	425.9			439.9			T (M1A)	
26				407.5			O-M1B-O	411

* Calculations based on a bulk modulus of 148 GPa (Comodi et al.,1992).
† δ corresponds to the in-plane bending mode where the atoms X-O-H remain in the plane during the bending.
‡ γ corresponds to the out-of-plane bending mode where the atoms X-O-H bend out of the plane.

TABLE 3. Far-IR bands and Mode Grüneisen parameters for triclinic chloritoid

	Fe-cld (MKM-97-8)				(Mg,Fe)-cld (RO1)				Mg-cld (MKM-98-43)				Mode	Raman
No.	ν_{i0} (cm^{-1})	$\delta\nu/\delta P$ (cm^{-1}/GPa)	$\delta^2\nu/\delta P^2$ (cm^{-1}/GPa^2)	γ_{i0} *	ν_{i0} (cm^{-1})	$\delta\nu/\delta P$ (cm^{-1}/GPa)	$\delta^2\nu/\delta P^2$ (cm^{-1}/GPa^2)	γ_{i0}*	ν_{i0} (cm^{-1})	$\delta\nu/\delta P$ (cm^{-1}/GPa)	$\delta^2\nu/\delta P^2$ (cm^{-1}/GPa^2)	γ_{i0}*		x_{Fe} = 0.59
27	382.6	1.786	0.099	0.71	383.0	3.788	–0.217	1.46	384.6	2.690		1.04	T (M2A), T (M2B)	
28	342.8	1.123		0.50	346.6	–1.555	0.382	–0.07	353.5	5.343	–0.229	2.24	R,T (Si)	343
29	328.5	0.079		0.04	329.0	0.546		0.25	329.5				T (M2A), T (M2B)	
30	318.8	4.329	–0.159	2.06	333.1	–1.840	0.500	–0.08	353.5				T (M1B)	
31									315.0				T (M2A), T (M2B)	
32									305.0				R,T (Si)	311
33	268.8	2.899		1.64	276.9	1.991		1.06	296.5			1.58	T (M1A)	
34									277.0	2.955			R, T (Si)	280
35	259.7	2.789		1.63	264.1	5.300	–0.327	2.97	269.7	4.007	–0.192	2.20	R, T (Si)	
36	252.7	2.117		1.27	253.6	1.923		1.12	256.7	2.475		1.43	R, T (Si)	258
37	241.4	2.448		1.54	246.4	1.911		1.15	251.2	2.508		1.48	R, T (Si)	
38	231.3	2.405	–0.048	1.58	231.9	1.948		1.24	235.4	1.068		0.67	T (M2A), T (M2B)	
39	158.0	1.716		1.65	192.7	1.901		1.46	205.1	3.834		2.77	T (M1B)	205
40	147.0	1.489		1.54					169.8				T (M1B)	
41	128.0	2.631	–0.185	3.12	133.4	8.023	–0.453	8.90	134.3	9.713	–0.574	10.70	T (M2A), T (M2B)	
42	96.7	0.308		0.48	98.3	0.348		0.52	109.9	0.499		0.67	T (M2A), T (M2B)	

* Calculations based on a bulk modulus of 148 GPa for a Mg-rich chloritoid (Comodi et al.1992)

and 3). These assignments are a first approximation as it is very likely that mode mixing occurs, but these should reflect the dominant atomic motion. Because of the close similarity of the IR spectra from the triclinic and monoclinic polymorphs (discussed below), we conclude that the frequencies of the two polarizations of the monoclinic form (A_u and B_u) are identical. Because of this behavior, bands are numbered starting with high frequency.

Triclinic end-member chloritoid. The two highest-frequency bands in the IR spectra (Fig. 1a) are assigned to stretching vibrations of the O1B-H1B and O1A-H1A dipoles, respectively (Table 2). The shoulders at the high-energy side of bands 1 and 2 of Fe-cld are most probably due to Fe^{3+} incorporation into M1A (Koch-Müller et al. 2000b). In Mg-cld the intense bands are shifted to higher energies, 3491 cm^{-1} (O1B-H1B) and 3057 cm^{-1} (O1A-H1A). For a partly deuterated (Fe,Mg) chloritoid solid solution (Fig. 1b), band 1 is shifted to 2570 cm^{-1} (ν_{OH}/ν_{OD} = 1.35) and band 2 to 2266 cm^{-1} (ν_{OH}/ν_{OD} = 1.32). The fine structure of the bands reflects changes in the atomic coordination of the protons due to Fe-Mg substitution, as is known to occur in amphiboles (Hawthorne 1981). Further study is needed for precise assignments.

The weaker band occurring at 2160 cm^{-1} (Fig. 1a) is clearly related to O-H (Koch-Müller et al. 2000b), but the number of

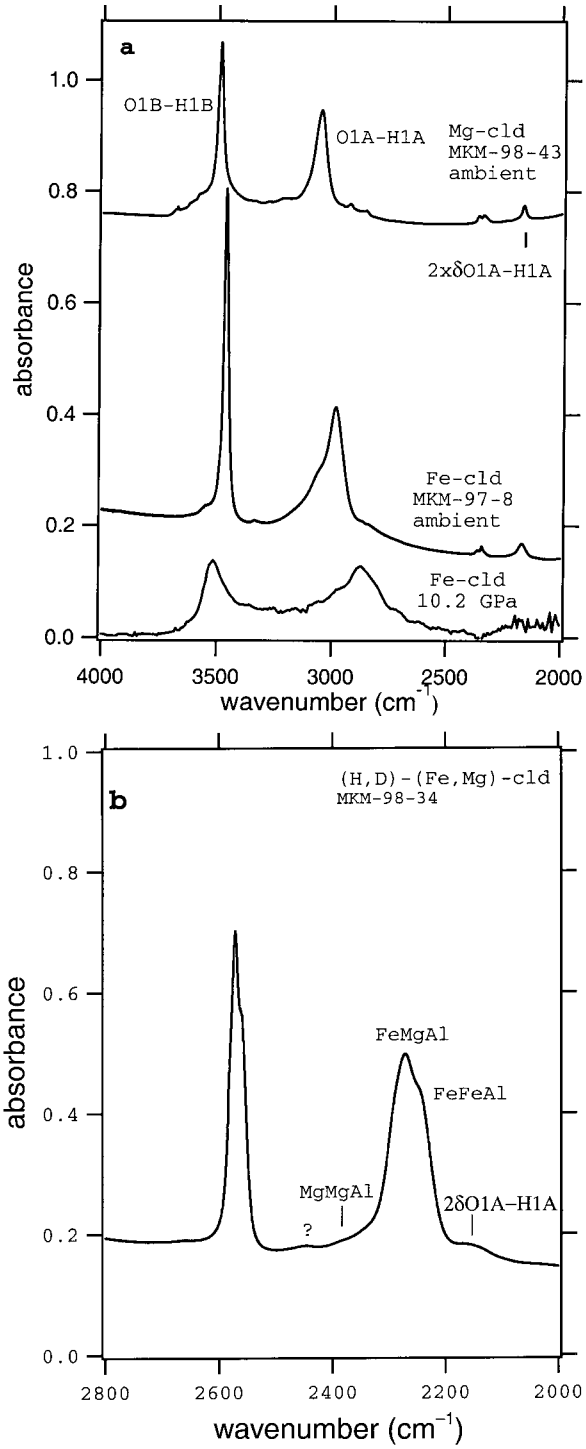

FIGURE 1. (**a**) O-H stretching bands of triclinic Mg-chloritoid at ambient conditions and of triclinic Fe-chloritoid at ambient conditions and at 10.2 GPa. The bands around 2300 cm^{-1} are due to stretching vibrations of atmospheric CO_2. (**b**) O-D stretching bands of a triclinic Fe, Mg chloritoid solid solution at ambient conditions. Spectra at ambient conditions were collected at the GeoForschungsZentrum Potsdam, those at high pressure were collected at the National Synchrotron Light Source, Brookhaven National Laboratory. The spectra are offset for clarity.

modes involving H is larger than expected from symmetry analysis. This fact coupled with the size of the pressure shifts (twice that of the fundamental, see below) allows assignment of the weak band to a first overtone of the bending $\delta_{O\text{-}H1A}$ at 1103 cm^{-1}.

The O-H bands broaden and shift upon compression (Fig. 1a). Our results to 10 GPa confirm (Fig. 2) the lower pressure measurements (to 2.8 GPa) of Koch-Müller et al. (2000b) wherein band 1 and the overtone (OT) shifted with pressure to higher frequencies whereas band 2 shifted to lower energies (Fig. 2). Frequency depends linearly on pressure with nearly the same slope for Fe- and Mg-cld (Fig. 2 and Table 2). The shift of band 2 to lower energies is in accordance with a shortening of the O1A-H1A····O2D distance of about 3% at 3.4 GPa (Comodi et al. 1992). The O1B-H1B dipole points into a triangle formed by O2C, O2A, and O2B. The distances between O1B and each of the O atoms in the triangle decrease with pressure by about 0.6% (Comodi et al. 1992). The pressure-shift of band 1 to higher energies was explained by Koch-Müller et al. (2000b). An increase in the bending angle of the O1B-H1B···O configuration leads to a weakening of the hydrogen bridge bonding (Hofmeister et al. 1999). However, up to now no refinement of the hydrogen atom positions, as a function of pressure, exists which could confirm this assumption.

To assign the O-H bending modes, we compared the spectrum of OH-bearing chloritoid with that of O(H,D)-bearing chloritoid (Fig. 3a). According to DeGrave et al. (1984), the in-plane vibrations ($\delta_{O\text{-}H1A}$ and $\delta_{O\text{-}H1B}$) are expected to occur at about 1100 and 700 cm^{-1}, respectively. The out-of-plane $\gamma_{O\text{-}H1A}$ vibrations should fall in the region 900–1000 cm^{-1} and $\gamma_{O\text{-}H1B}$ is expected at about 800 cm^{-1}. The response of the IR spectra

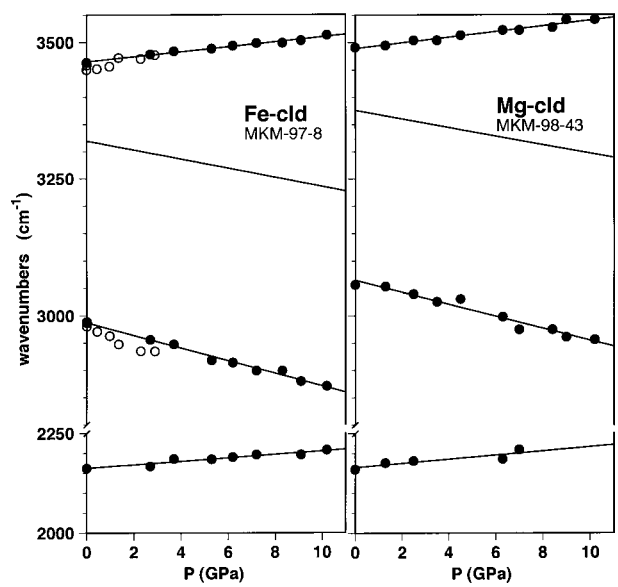

FIGURE 2. Band positions of the O1B-H1B and O1A-H1A-stretching vibrations of Fe- and Mg-chloritoid as a function of pressure. The solid circles are the results of this study; the open circles were taken from Koch-Müller et al. (2000b).

upon substitution of D for H confirms the assignments for the bending modes (Fig. 3a and Table 2). Thus, band 3 is assigned to $\delta_{O\text{-}H1A}$ (ν_{OH}/ν_{OD} = 1.36), band 7 is not quite clear and is preliminary assigned to $\gamma_{O\text{-}H1A}$ (ν_{OH}/ν_{OD} = 1.30), band 10 and band 13 are assigned to $\gamma_{O\text{-}H1B}$ (ν_{OH}/ν_{OD} = 1.25) and $\delta_{O\text{-}H1B}$ (ν_{OH}/ν_{OD} = 1.25), respectively.

In the mid-IR region, altogether 24 different modes could be detected for the various compositions (Fig. 3b). All the bands except for band 3 shift to higher frequency with increasing Mg content. Bands observed in the Fe-chloritoid as shoulders are well resolved in the Mg-chloritoid spectra due to this compositional shift. There is a linear relationship between the peak position of the bands and chemical composition (Fig. 4). As expected, the changes in the wavenumbers as a function of composition are different for the different bands and were used to assign the bands (Table 2 and Fig. 4).

The peaks in mid-IR spectra of Fe-chloritoid broadened as the pressure was increased to 10.2 GPa (Fig. 5). We were only able to analyze the pressure-shifts for the strongest and/or isolated bands (Table 2). Because the band broadening was only observed in the mid-IR spectra and not in the near- or far-IR spectra, it is not due to changes in the crystal structure. The bands shift with increasing pressure to higher frequency at various rates (Fig. 6). In principal, bands belonging to the same motion should show the same pressure dependence for the Mg and Fe end-members. However, the magnitudes of the slope of $\partial\upsilon_i/\partial P$ for some of the bands of Fe-chloritoid are smaller than those for Mg-chloritoid.

All of the bands in the far-IR spectra shift toward higher frequency with increasing Mg content (Figs. 7 and 8), as expected, but to a varying degree. For most of the bands, frequency depends linearly on composition, but for some bands a non-linear fit is needed (Table 3).

For the far-IR region, the response of different chloritoid compositions to pressure was investigated. Spectra of Fe-chloritoid are shown as an example in Figure 9. The far-IR bands increase in frequency with pressure (Fig. 10). Bands

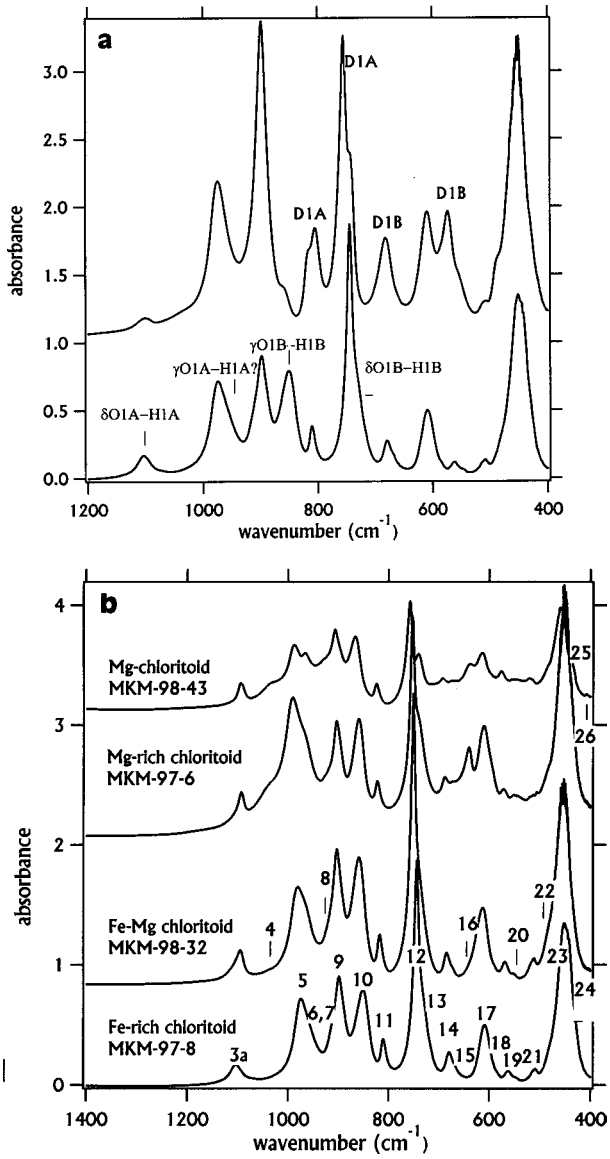

FIGURE 3. (**a**) Mid-IR spectrum of a triclinic O(D,H)-bearing chloritoid, MKM-98-34, (top) in comparison to a spectrum of a triclinic OH-bearing chloritoid, MKM-98-31. (**b**) Mid-IR spectra of triclinic OH-bearing chloritoids of different compositions. The spectra were collected at the GeoForschungsZentrum Potsdam.

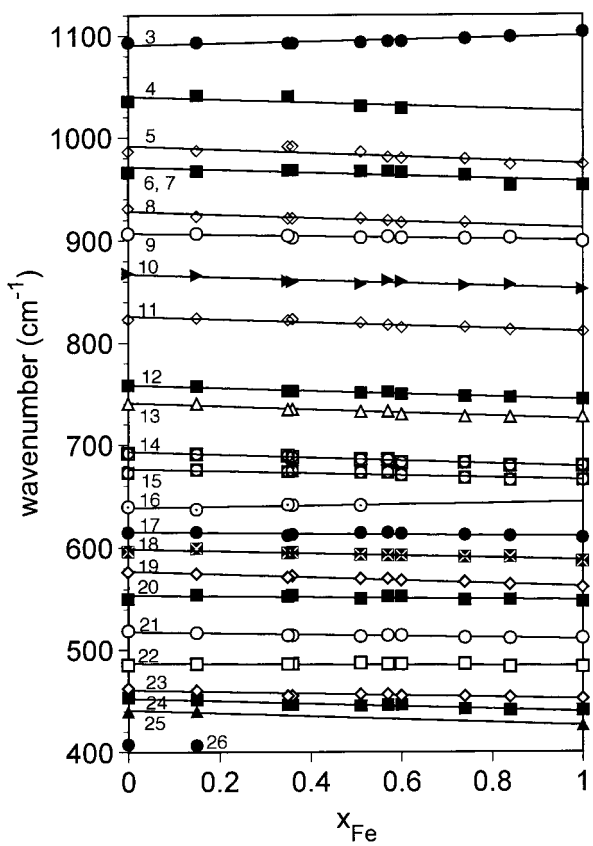

FIGURE 4. Positions of the mid-IR bands in chloritoid as a function of composition.

which arise from the same atomic motion should show a similar pressure dependence for the three compositions. Such behavior is observed, but the magnitude of the slope of $\partial\upsilon_i/\partial P$ for some bands decreases with increasing x_{Fe}.

IR spectra of a natural monoclinic chloritoid. The IR spectrum of a natural, monoclinic Fe-rich chloritoid between 400 and 4000 cm^{-1} appears similar to spectra of triclinic Fe-rich chloritoids in Figure 3. From the symmetry analysis, however, all bands should split (Table 1). Splitting is observed only for the one band near 610 cm^{-1} in triclinic chloritoid, which splits into two bands at 614 and 590 cm^{-1} in the spectrum of the monoclinic sample. This splitting was observed by Moenke (1962) and De Grave et al. (1984) and was attributed to the difference in the symmetry of monoclinic and triclinic chloritoid. We conclude that the frequencies of the two polarizations (A_u and B_u) of the monoclinic form for all other bands are identical.

Band assignments

The assignments of bands 1, 2, 3 (and its overtone OT), 7, 10, and 13 have already been discussed in the previous sections. For the assignment of the other bands the strategy outlined below has been applied. The number of expected vibrations for the different motions can be taken from Table 1. The energy ranges of the specific vibrations given below are

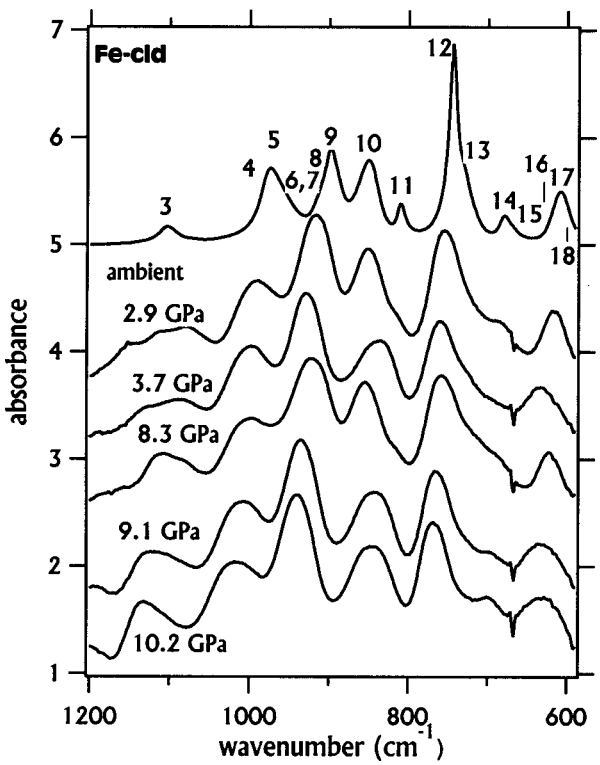

FIGURE 5. Mid-IR spectra of Fe-chloritoid (MKM-97-8) at different pressures collected at the National Synchrotron Light Source, Brookhaven National Laboratory.

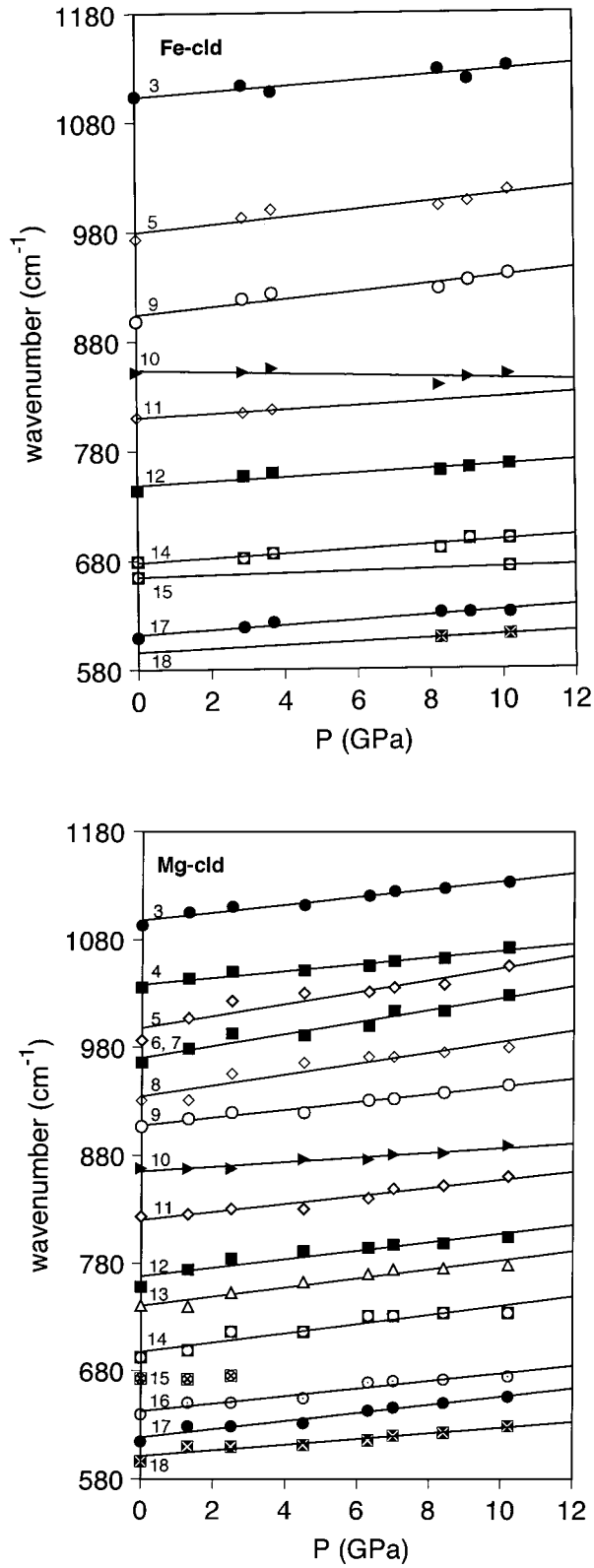

FIGURE 6. Positions of the mid-IR bands in Fe-chloritoid (**a**) and Mg-chloritoid (**b**) as a function of pressure.

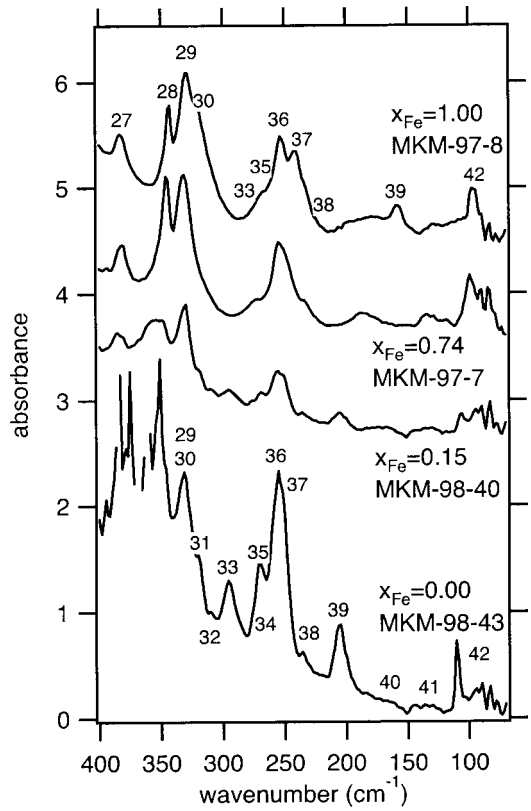

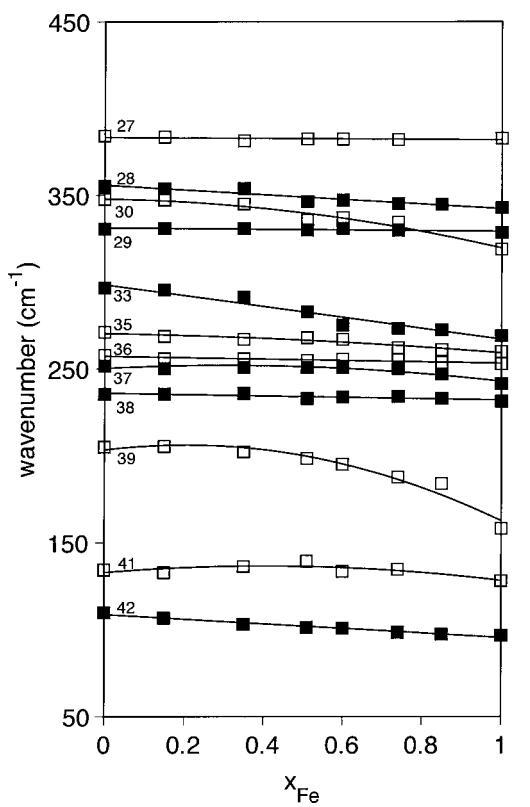

FIGURE 8. Positions of the far-IR bands in chloritoid as a function of composition.

◀ **FIGURE 7.** Far-IR spectra of chloritoid of different compositions collected at the National Synchrotron Light Source, Brookhaven National Laboratory. The spectrum of the Mg-chloritoid was taken on a very thick sample (estimated thickness 50 μm) to enhance the weakest bands. As a consequence the very intense bands at wavenumbers greater 350 cm^{-1} are off-scale. The spectra are offset for clarity.

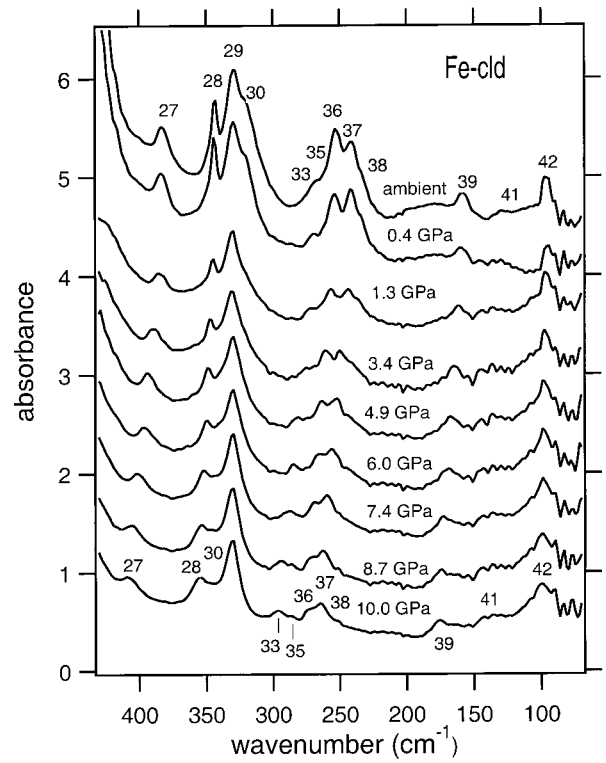

FIGURE 9. Far-IR spectra of Fe-chloritoid at different pressures. The spectra were collected at the National Synchrotron Light Source, Brookhaven National Laboratory. The spectra are offset for clarity.

taken from Farmer (1974) and De Grave (1984).

Strategy of the band assignment:

(1) Vibrations involving the Fe and/or Mg bearing M1B octahedron should depend strongly on both composition and pressure. The three O-M1B-O stretching and three O-M1B-O bending vibrations are expected to occur between 400 and 1000 cm^{-1}. The three translatory vibrations of the M1B cations are expected below 400 cm^{-1}.

(2) Vibrations involving the Al-bearing M1A octahedron should depend weakly on composition, but strongly on pressure. Al-O stretching vibrations are expected in the range of 600–700 cm^{-1} and the translatory vibrations of the Al cations below 450 cm^{-1}.

(3) Vibrations of the Al-bearing octahedra of the L2 layer should depend weakly on both composition and pressure.

(4) Vibrations of the SiO_4 tetrahedra that connect the more compressible layer L1 with the rigid layer L2 should depend

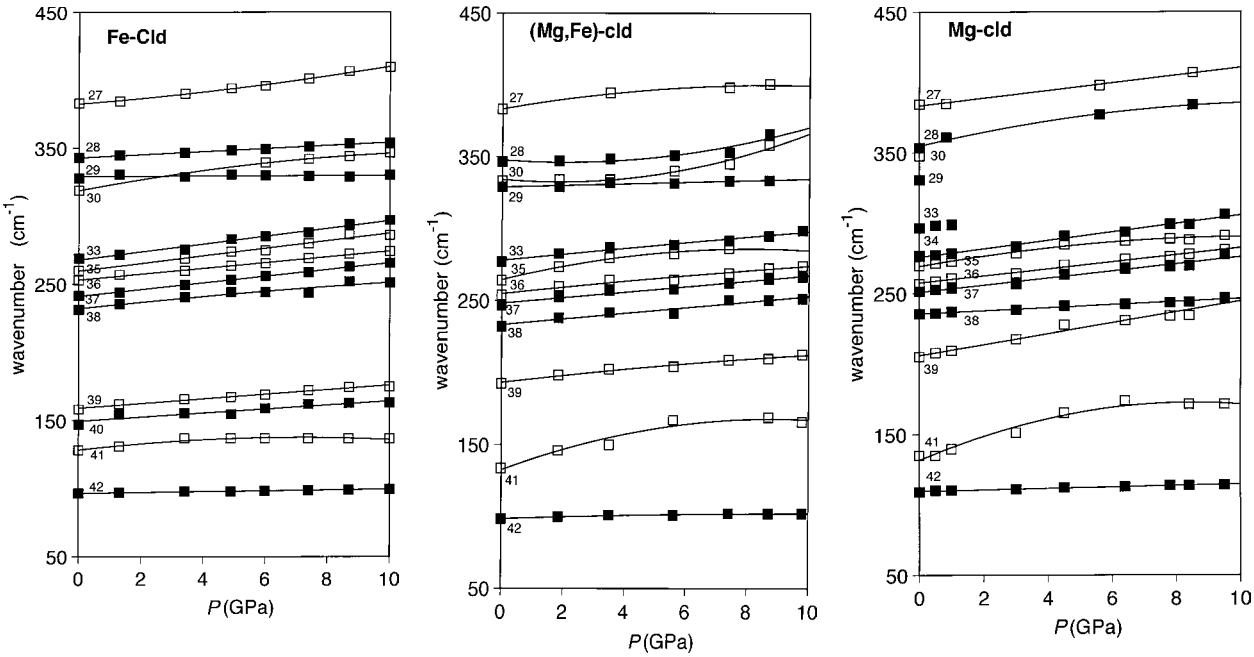

FIGURE 10. Positions of the far-IR bands in Fe-chloritoid (**a**), Fe-Mg-chloritoid (RO1) (**b**) and Mg-chloritoid (**c**) as a function of composition.

weakly on both composition and pressure. The Si-O stretching vibrations ν_1 and ν_3 usually occur at energies between 700 and 1200 cm^{-1}, O-Si-O bendings ν_2 and ν_4 between 400 and 600 cm^{-1}, and the translatory and rotational vibrations below 400 cm^{-1}.

Raman spectra

Raman spectra of silicates are commonly less intense than IR spectra, resulting in the observation of only 21 of the expected 33 Raman-active bands in the spectrum of a triclinic natural chloritoid (Table 2 and 3). The frequencies of most of the Raman bands resemble the frequencies of the IR bands, and correlate with IR bands assigned to motions of the SiO_4 tetrahedron. Frequencies corresponding to modes in the IR that were assigned to translations involving the Al-bearing M1A, M2A, and M2B (M2B1 and M2B2) are not observed. This result is consistent with the analysis in Table 1. The translation of the M1B cation is active in the Raman, consistent with the observation of a band at 205 cm^{-1}.

PRESSURE DEPENDENCE OF THE VIBRATIONAL MODES

Mode Grüneisen parameters calculated from:

$$\gamma_i = \frac{K_T}{\nu_{i0}} \frac{\partial \nu_i}{\partial P} \quad (1)$$

are listed in Tables 2 and 3. We used the bulk modulus determined by Comodi et al. (1992) in the calculations of the Grüneisen parameters. The bulk modulus was determined in a diamond-anvil cell from a single-crystal of magnesiochloritoid (x_{Mg} = 0.65) at 148 GPa. There are two other studies which used powdered chloritoid samples to determined the bulk moduli of chloritoid (Grevel 2000; Theye 2000). Both were performed at HASYLAB (Hamburg) using the MAX 80 multi-anvil device. Grevel (2000) determined the bulk modulus of a synthetic magnesiochloritoid end-member (x_{Mg} = 1.0) K_T = 127.7 ± 2.4 GPa. Theye (2000) determined the bulk moduli of two natural Fe-Mg chloritoid with x_{Mg} = 0.1 (K_T = 153 ± 8 GPa) and with x_{Mg} = 0.48 (K_T = 123 ± 2 GPa). Because there is no trend of K_T as a function of composition detectable in these data, we used the single-crystal data by Comodi et al. (1992) to calculate γ_i, independent of the compositions of the chloritoids.

The γ_i values related to the internal modes are significantly smaller than those of the external modes (Tables 2 and 3). This behavior has also been observed for other materials such as olivine and has been attributed to the incompressibility of the Si-O bonds compared to the more compressible MgO_6 octahedra (e.g., Hofmeister et al. 1989). For olivine the average γ_i for the internal modes is 0.46 and for the external modes is 1.32. However, for wadsleyite Cynn and Hofmeister (1994) observed that only a few of their internal modes have low values for γ_i; most have values close to unity, indicating that the vibrating units in wadsleyite respond quite uniformly to the increase in pressure.

The macroscopic or thermodynamic Grüneisen parameter, γ_{th}, is defined by

$$\gamma_{th} = \frac{K_T \alpha V}{c_v} \quad (2)$$

where V is the volume, and α is the thermal expansivity. The mode Grüneisen parameter γ_i is related to the thermodynamic Grüneisen parameter by

$$\gamma_{th} = \frac{\sum \gamma_i C_{v,i}}{\sum C_{v,i}} \quad (3)$$

where $C_{V,i}$ is the contribution of the i^{th} vibrational mode to the total specific heat. In a first approximation a simple average of the mode Grüneisen parameters $\langle\gamma_i\rangle$ can be used to calculate

γ_{th} (Hofmeister and Mao 2002). However, as outlined in Hofmeister and Mao (2002), and previously, this average $<\gamma_i>$ is up to 25% lower than the thermal Grüneisen parameter obtained from thermodynamic quantities. According to Hofmeister and Mao (2002) this discrepancy arises because Equation 1 is valid only for monatomic and diatomic solids. They redefined γ_i and proposed to use the appropriate polyhedral bulk moduli, K_x, instead of the bulk modulus K_T in Equation 1. We observe the same tendency for chloritoid: the average $<\gamma_i>$ =1.25 for magnesiochloritoid is 17% lower than γ_{th} = 1.51 using the thermodynamic quantities obtained in this study and the α value as determined by Ivaldi et al. (1988).

Hofmeister et al. (1999) observed a linear increase of the pressure derivatives of hydroxyl bands with peak position for several different phases. Compressible phases show a steep slope while the slope for incompressible phases such as wadsleyite is relatively shallow. The pressure derivatives of the hydroxyl bands in chloritoid follow the trend observed by Hofmeister et al. (1999): $(\partial\upsilon_l/\partial P)$ increases linearly with band position; $(\partial\upsilon_l/\partial P) = -113.29 + 0.034\nu$ for Fe-chloritoid and $(\partial\upsilon_l/\partial P) = -124.86 + 0.037\nu$ for Mg-chloritoid, where ν is in cm^{-1} and P is in GPa. According to Hofmeister et al. (1999) the trends are correlated to the bulk moduli of the phases. The trend for chloritoid (K_T = 148 GPa, Comodi et al. 1992) has steeper slope than that of wadsleyite (K_T = 174 GPa, Weidner et al. 1984) but a flatter slope than that of coesite (Koch-Müller et al. 2001) (K_T = 96 GPa, Levien and Prewitt 1981) and brucite (K_T = 42 GPa, Duffy et al. 1995).

As mentioned before the pressure derivatives for the IR bands are higher for the Mg-end-member than for the Fe-end-member. This suggests that the Mg-end-member is more compressible than the Fe-end-member. This assumption seems to be reasonable because the M1B octahedron in Mg-chloritoid is larger than is necessary to incorporate the small Mg ion (Ivaldi et al. 1988).

VIBRATIONAL MODELING OF C_P AND S_o

Kieffer (1979, 1980) developed a model based on lattice dynamics that allows calculation of C_V and S_o from vibrational frequencies and acoustic velocities. The three acoustic modes are treated as Debye oscillators. For the optic modes, a density of states [g(ν)] is constructed by grouping similar modes together either as delta functions (Einstein oscillators) or as blocks of frequency (optic continua). As suggested by our data, we assumed that Raman bands have the same frequencies as the IR bands that originate from similar motions (Table 1).

The calculations can be compared to calorimetric data via the anharmonic correction:

$$C_P = C_V + TV\,\alpha^2 K_T \text{ and } S_o = S_V + TV\,\alpha^2 K_T \quad (4)$$

The heat capacities and entropies for the triclinic polymorphs of Fe- and Mg-chloritoid were calculated using a Kieffer-type model with four Einstein oscillators (O-H stretching and bending modes), three Debye oscillators (acoustic modes) and nine continua for the optical modes (Fig. 11, Table 4). The acoustic modes were estimated as v_S = 5 km/s and v_P = 9 km/s from elastic data on compounds with similar densities and bulk moduli (see Bass 1995).

The calculated heat capacity data for triclinic Mg- and Fe-chloritoid based on the formula $M_2Al_4O_2(SiO_4)_2(OH)_4$ were fit to the polynomial expressions J/(mol·K) for

$$C_P = 7.835 \cdot 10^2 - 5.170 \cdot 10^3 T^{-0.5} - 1.648 \cdot 10^7 T^{-2} + 1.934 \cdot 10^9 T^{-3} \text{ (Mg-cld)} \quad (5)$$

$$C_P = 7.848 \cdot 10^2 - 5.185 \cdot 10^3 T^{-0.5} - 1.548 \cdot 10^7 T^{-2} + 1.783 \cdot 10^9 T^{-3} \text{ (Fe-cld)} \quad (6)$$

Both equations are valid for $T > 298.15$ K (Figs. 12a and 12b). The calculated third law entropies are S_o J/(mol·K) = 293 (Mg-cld) and 335 (Fe-cld) (Table 5). The value for Fe-cld includes the ideal magnetic contribution for two Fe^{2+}atoms pfu, $S_{mag} = 2 * R \ln(2s + 1) = 26.76$ J/(mol·K), with s = spin quantum number = 2 (Ulrich and Waldbaum 1976). According to the results of Koch-Müller et al. (2000a) no electronic contribution to the entropy has to be added since the M1B site in chloritoid, in which Fe^{2+} is incorporated, is highly distorted. This leads to a splitting of the T_{2g} groundstate into three different energy levels with the sixth electron of Fe^{2+} in the lowest energy level. Therefore the electronic entropy is zero. Finally, the heat capacities and entropies for the monoclinic polymorphs of Fe- and Mg-chloritoid were calculated. As expected from the similarity of the spectra the difference in the heat capacity and entropy data for the monoclinic and triclinic polymorph is negligible and is not shown here.

DISCUSSION OF THE THERMODYNAMIC DATA

Neither C_P nor S_o of chloritoid has been directly measured, but these values have been obtained by refining thermodynamic databases (Gottschalk 1997; Simon et al. 1997; Chatterjee et al. 1998; Vidal et al. 1999) or were estimated on the basis of the Neumann-Kopp rule (Helgeson et al. 1978; Holland 1989; Holland and Powell 1998). Table 5 compares the thermodynamic data from the literature with those obtained in this study. For Mg-cld, the entropy obtained in this study [293 J/(mol·K)] is slightly higher than the values reported in the literature: S_o J/(mol·K) = 284 (Vidal et al. 1999) and 264 (Holland and Powell 1998; Simon et al. 1997). The entropy for Fe-cld [335 J/

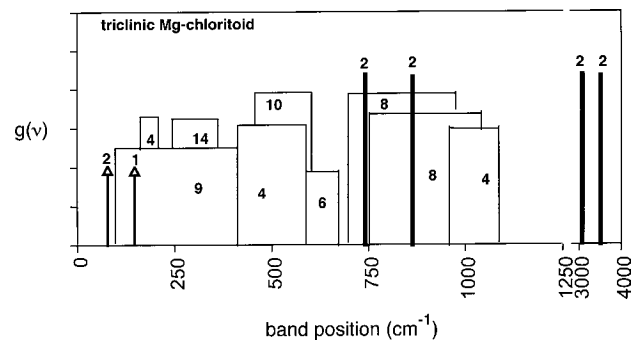

FIGURE 11. Optical density of state for triclinic Mg-chloritoid. The heavy lines represent the Einstein oscillators (O-H stretching and bending modes), the arrows the Debye oscillators (acoustic modes) and the rectangles the continua (remainder optical modes). The numbers refer to the numbers of oscillators.

TABLE 4. Density of states for chloritoid

Assignment	No. of modes monoclinic	No. of modes triclinic	Band position Mg-cld cm^{-1}	Band position Fe-cld cm^{-1}	IR-bands
O-H stretching	4	2	3490	3463	1
O-H stretching	4	2	3057	2989	2
X-O-H bending	8	4	1090–960	1100–952	3, 7
$\nu_3 + \nu_1$	16	8	1040–750	1030–740	4, 9, 11, 12
X-O-H bending	4	2	868	852	10
X-O-H bending	4	2	741	727	13
O-Mg-O stretching O-Mg-O bending	16	8	970–690	960–680	14, 8, 6, 5
Al-O stretching	12	6	670–580	665–570	15, 16, 17
$\nu_4 + \nu_2$	20	10	600–455	590–445	18, 20, 21, 22, 23
O-Mg-O bending	8	4	580–403	570–380	19, 26
T (M2A), T (M2B), T (M1A)	21	9	460–100	450–90	24, 25, 27, 29, 31, 33, 38, 41, 42
R, T (Si); T (M1B)	28	14	360–250	350–240	28, 30, 32, 34, 35, 36, 37,
T (M1B)	8	4	210–165	165–145	39, 40
LA	1	1	155	154	
TA	2	2	86	85	

Notes: For the optic modes, a single frequency (in cm^{-1}) was assumed to be dispersed as an Einstein oscillator, whereas the range of frequencies indicates an optic continuum. See Kieffer (1979) for details. Parameters common to all phases are: thermal expansivity $\alpha = 30 \times 10^{-6}$ /K; isothermal bulk modulus $K_{T_r} = 148$ GPa; dK/dP = 4.

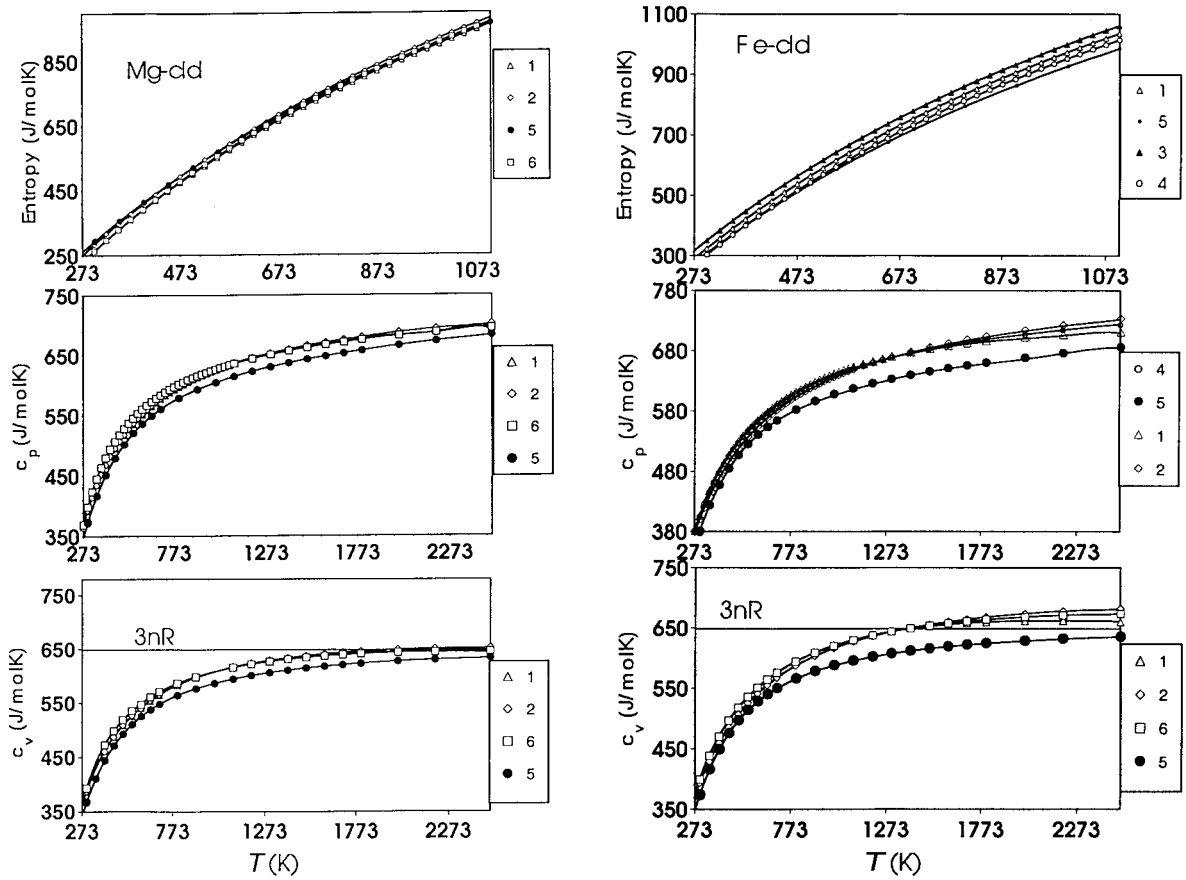

FIGURE 12. Entropy S_o and heat capacities, C_P and C_V for Mg-chloritoid (**a**) and Fe-chloritoid (**b**) obtained in this study in comparison with literature data: (1) Holland and Powell 1998; (2) Vidal et al. 1999; (3) Gottschalk (1997); (4) Chatterjee et al. (1998); (5) this study; (6) Simon et al. (1997).

(mol·K)], is 9% higher than the refined value of S_o = 303 J/(mol·K) (Chatterjee et al. 1998) but 5% lower than the estimated S_o = 352 J/(mol·K) (Helgeson et al. 1978). Holland and Powell (1998) used the model developed by Holland (1989) to estimate the entropy for Fe- and Mg-chloritoid and fixed these values in their database to refine H_f for the phases involved. The Neumann-Kopp rule (the basis for this model) allows the estimation of the entropies of complex compounds by summing the entropies of simpler chemical entities, such as elements or oxides. Holland (1989) showed that the volume of a phase and the coordination state of the cation polyhedra have an effect on the entropy and introduced an entropy-volume-

TABLE 5. Comparison of entropy, heat capacity (J/mol·K) and enthalpy (kJ/mol) data for triclinic Fe- and Mg-chloritoid [$(M_2Al_4O_2(SiO_4)_2(OH)_4$]

Reference	Fe–cld					Mg–cld				
	S_o	H_f	C_P			S_o	H_f	C_P		
			298	500	700			298	500	700
Holland and Powell (1998)	324 *	–6418 (2) *	404	527	589	264	–7119(2)	393	578	614
Vidal et al. (1999)	324	–6422	399	517	581	284	–7100	393	518	578
Simon et al. (1997)	–	–	–	–	–	264	–7115	369	528	584
Gottschalk (1997)	350 (<1)	–6393 (<1)	– †	– †	– †	–	–	–	–	–
Helgeson et al. (1978)	352	–	422	533	584	–	–	–	–	–
Chatterjee et al. (1998)	303 (6)	–6437 (6)	405	528	589	–	–	–	–	–
this study	335 (9) §	–6422 ‡	378	505	562	293(9)	–7101 ‡	367	493	548

* The data in the latest data file HP98 differ slightly: H_f = 6424 and S_o = 316.
† Not refined, taken form Holland and Powell (1990).
‡ Estimated in order to fit the experimental data in combination with compressibility data of Comodi et al. (1992) and thermal expansion of Ivaldi et al. (1988).
§ S_o plus the ideal magnetic contribution $S_{mag} = n$R ln(2s+1) with s = spin quantum number = 2 (Fe^{2+}) and n = Fe^{2+} atoms pfu.

coordination model. According to this model the entropy of phase j can be calculated as $S_j = V_j + \Sigma n_i(S_i - V_i)$, whereas V_j is the volume of phase j, S_i and V_i are the entropies and volumes of oxide components i, which are present in amount n_i and in the same coordination state as in the mineral. The values of $(S_i - V_i)$ were determined by least squares analyses from measured entropies of oxides and silicates. When applying this model to chloritoid some difficulties have to be overcome. (1) Which $(S_i - V_i)$ value for H_2O should be used. Holland (1989) gives data for a high-entropy and low-entropy H_2O group; the data for the high-entropy group should be used for OH groups with weak hydrogen bonds and large degree of freedom and the data for the low-entropy group should be used for OH groups with strong hydrogen bonds. (2) For Fe^{2+}-cld magnetic order-disorder has to be considered; in his prediction of entropies Holland (1989) added the ideal magnetic contribution to the calculated entropy values: $S_{mag} = n$R ln(2s + 1) with s = spin quantum number = 2(Fe^{2+}) and n = Fe^{2+} atoms pfu. (3) For Fe^{2+}-cld differences in the degree of disorder of the sixth electron in oxide component FeO and in the corresponding Fe^{2+} polyhedra may contribute to the overall entropy (see Wood 1981).

Holland (1989) suggested for Mg-chloritoid an entropy value of $S_{Mg_2Al_4O_2(SiO_4)_2(OH)_4} = V_{Mg_2Al_4O_2(SiO_4)_2(OH)_4} + 2 * (S-V)_{MgO} + 2 * (S-V)_{Al_2O_3} + 2 * (S-V)_{SiO_2} + 2(S-V)_{H_2O(b)} = 264 \pm 4$ J/(mol·K) which is about 11% lower than the value obtained in this study [(293 ± 9 J/(mol·K)]. In his calculations Holland (1989) considered H_2O in chloritoid to belong to the low-entropy group. This may be true for the strongly hydrogen bonded O1A···H1A dipole but not for the O1B···H1B dipole which shows nearly no hydrogen bonding to the tetrahedral layer. In addition there is a large degree of freedom because the dipole O1B···H1B points directly into a triangle formed by the O2C, O2A, and O2B atoms and all three O atoms are supposed to be the acceptors for the weak hydrogen bonding. Thus, splitting the $2(S-V)_{H_2O(b)}$ value in $1(S-V)_{H_2O(a)}$ and $1(S-V)_{H_2O(b)}$ would increase the calculated entropy to 272.4 ± 4 J/(mol·K).

For Fe-chloritoid Holland (1989) suggested an entropy value of $S_{Fe_2Al_4O_2(SiO_4)_2(OH)_4} = 324 \pm 4$ J/(mol·K) which is about 3% lower than the value obtained in this study [335 ± 9 J/(mol·K)]. Following the explanation given above for the different water groups in chloritoid the entropy would be 331.4 J/(mol·K). This value is in good agreement with the value obtained in this study, which is somehow surprising since this value contains a term for the magnetic contribution to the entropy but no correction for the electronic contribution was made. However, Fe^{2+} in FeO occupies a nearly regular octahedron while Fe^{2+} in Fe-cld is located in a highly distorted octahedral site. To correct this entropy value for the electronic contribution of Fe^{2+} in FeO one should subtract 18.2 J/(mol·K) (for 2 Fe^{2+}) from the value given by Holland (1989). Helgeson et al. (1978) estimated the entropy for Fe-cld as 352 J/(mol·K) using an oxide summation type algorithm. They corrected the entropies for all Fe-bearing minerals by subtraction n * 8.836 J/(mol·K) from the summation value (n = number of moles of ferrous iron). But no correction for the magnetic contribution has been made. Thus, the published entropy data for Fe-cld, although estimated using a similar algorithm, are not consistent and the data presented here are more reliable.

In Figure 12 we compare the entropy and specific heat at constant volume calculated from published C_P data using the relation $C_V = C_P - \alpha^2 V K_T T$ with the entropy and C_V data obtained by vibrational modeling. For the entropy of Mg-cld as a function of temperature there is an excellent agreement between the calculated and estimated data. The published entropy data for Fe-chloritoid range from 303 to 352 J/(mol·K) at ambient conditions. Our entropy value is with 335 J/(mol·K) within this range. For the specific heat at constant volume of Fe-cld the literature data cross the harmonic Dulong and Petit limit ($3n$R = 648 J/(mol·K) for chloritoid) at about 1300 K. For Mg-cld, however, the published C_V values tend toward the limit. The C_V values for Fe- and Mg-cld calculated under harmonic assumptions with the density of state stay below the limit (Figs. 12a and 12b). Crossing the harmonic Dulong and Petit limit could indicate an intrinsic mode anharmonicity. However, if the modes are strongly anharmonic it should apply for both end-members, Fe- and Mg-cld. Thus, the published C_V values for Fe-cld may be overestimated.

Using our new values for Mg-cld in combination with an enthalpy of formation of H_f = –7101 kJ/mol and the compressibility data and thermal expansion data of chloritoid as determined by Comodi et al. (1992) and Ivaldi et al. (1988), respectively, we reproduced the experimental data of the reaction Mg-chloritoid + talc = clinochlore + kyanite (Chopin 1985) very well (Fig. 13a). For Fe-cld a similar exercise can be performed using the experimental data points of reaction Fe-chloritoid = almandine + diaspore + water (Vidal et al. 1994) (Fig. 13b). Our thermodynamic data for Fe-chloritoid in combination with H_f = 6422 kJ/mol and the compressibility and

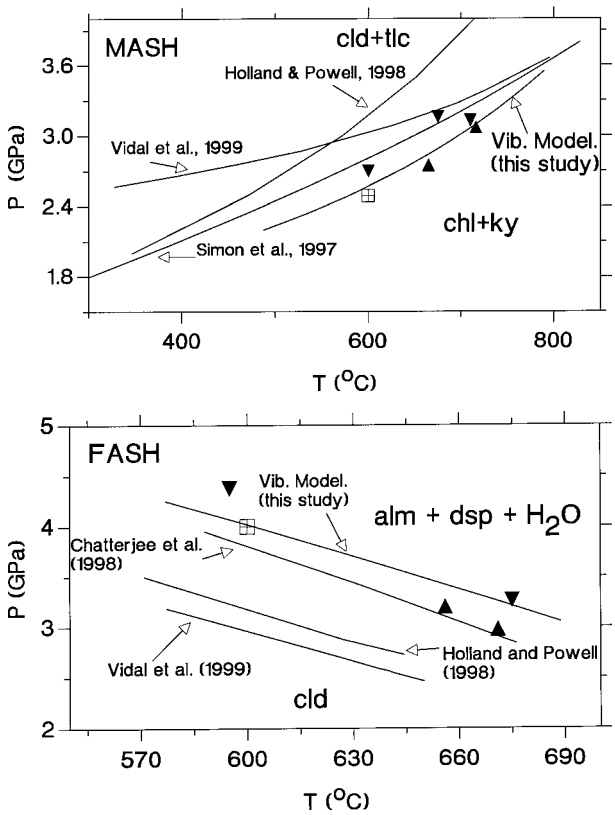

FIGURE 13. Pressure-temperature diagrams showing the reaction Mg-cld + tlc = chl + ky reaction (**a**) and the reaction Fe-cld = alm + dsp + H_2O (**b**) calculated with the Thermocalc software and database (Holland and Powell 1998), the Bayes software and database (Chatterjee et al. 1998) and the GEOCalc software (Brown et al. 1988) but using the thermodynamic data derived by Simon et al. (1997), Vidal et al. (1999) and in this study (Vib. Model). The triangles and inverted triangles show the experimental brackets of Chopin et al. (1995) (**a**) and Vidal et al. (1994) (**b**). The crossed square in both figures refers to the presence of all 4 phases after the experiments. Abbreviations after Kretz (1983).

thermal expansion data mentioned above reproduce the experimental phase equilibrium data very well. However, the enthalpy data given above are only estimated in order to fit the experimental brackets. In this estimate we assumed ideal end-member compositions for the coexisting phases that may not be true for chlorite, talc, and/or Fe-chloritoid in these experiments. For example, Vidal et al. (1994) state that the Fe-cld used in their experiments may contain Fe^{3+} that would shift the equilibrium to higher temperature. Thus, the enthalpy data need to be further refined to be consistent with other experimental results.

ACKNOWLEDGMENTS

We thank T. Mock for the help with the heavy liquid separation. R.J. Hemley, A. Gonscharov, E. Gregoryanz, H.K. Mao, and V. Strutzkin are thanked for helpful comments and advice. The comments of the reviewers C. Bertoldi and O. Vidal improved the paper. M.K.M. thanks Franz-Josef Müller for his steady support and encouragement. This research was supported by the N.S.F. Center for High Pressure Research, N.S.F. grants (EAR-9873577 and EAR 0079510), and the Carnegie Institution of Washington.

REFERENCES CITED

Bass, J.D. (1995) Elasticity of minerals, melts, and glasses. In Ahrens T.J., Ed., Handbook of physical constants. American Geophysical Union, Special Publication, V 61.2, 45–63. Washington, D.C.

Brindley, G.W. and Harrison, F.W. (1952) The structure of chloritoid. Acta Crystallographica, 5, 698–699.

Brown, T.H., Berman, R.G., and Perkins, E.H. (1988) GeO-Calc: software package for calculation and display of pressure-temperature-composition phase diagrams using an IBM or compatible personal computer. Computers in Geoscience, 14, 279–289.

Chatterjee, N.D., Krüger, R., Haller, G., and Olbricht W. (1998) The Bayesian approach to an internally consistent thermodynamic database: theory, database, and generation of phase diagrams. Contribution to Mineralogy and Petrology, 133, 149–168.

Chopin, C. (1983) Magnesiochloritoid, a key-mineral for the petrogenesis of high-grade pelitic blueschists. Bulletin de Minéralogie, 106, 715–717.

———(1985) Les relations de phases dans les metapelites de haute pression. PhD Thesis. Mémoires des Sciences della Terre, Université Pierre et Marie Curie, Paris, no. 85-11, pp. 80.

Chopin, C. and Monié, P. (1984) A unique magnesiochlortoid-bearing, high-pressure assemblage from the Monte Rosa, Western Alps: petrologic and ^{40}Ar-^{39}Ar radiometric study. Contribution to Mineralogy and Petrology, 87, 388–398.

Chopin, C., Seidel, E., Theye, T., Ferraris, G., Ivaldi, G., and Catti, M. (1992) Magnesiochloritoid, and the Fe-Mg series in the chloritoid group. European Journal of Mineralogy, 4, 67–76.

Comodi, P., Mellini, M., and Zanazzi, P.F. (1992) Magnesiochloritoid: compressibility and high pressure structure refinement. Physics and Chemistry of Minerals, 18, 483–490.

Cynn, H. and Hofmeister, A.M. (1994) High-pressure IR spectra of lattice modes and OH vibrations in Fe-bearing wadsleyite. Journal of Geophysical Research, 99, 17717–17727.

Cynn, H., Hofmeister, A.M., Burnley, P.C., and Navrotsky A. (1996) Thermodynamic properties and hydrogen speciation from vibrational spectra of dense hydrous magnesium silicates. Physics and Chemistry of Minerals, 23, 361–376.

De Grave, E., Vanleerberghe, R., Verdonck, L., and De Geyter, G. (1984) Mössbauer and infrared spectroscopic studies of Belgian chloritoids. Physics and Chemistry of Minerals, 11, 85–94.

Duffy, T.S., Shu, J., Mao, H.-K., and Hemley, R.J. (1995) Single-Crystal X-ray diffraction of brucite to 14 GPa. Physics and Chemistry of Minerals, 22, 277–281.

Farmer, V.C. (1974) The infrared spectra of minerals. Mineralogical Society Monograph 4, Mineralogical Society London, p. 539.

Farmer, V.C. and Lazarev, A.N. (1974) Symmetry and Crystal Vibrations. In Farmer V.C., Ed., The infrared spectra of minerals. Mineralogical Society Monograph 4, Mineralogical Society London, p. 539.

Fransolet, A.-M. (1978) Donnée nouvelles sur l'ottrélite d'Ottré, Belgique. Bulletin de Minéralogie, 101, 548–557.

Ganguly, J. (1969) Chloritoid stability and related parageneses: theory, experiments and applications. American Journal of Science, 267, 910–944.

Gottschalk, M. (1997) Internally consistent thermodynamic data for rock forming minerals in the system SiO_2-TiO_2-Al_2O_3-Fe_2O_3-CaO-MgO-FeO-K_2O-Na_2O-H_2O-CO_2. European Journal of Mineralogy, 9, 175–223.

Grevel, K.D. (2000) P-V-T data of hydrous high-pressure phases. Eos, Transactions of the American Geophysical Union, 81, p. 1150.

Hanscom, R.H. (1975) Refinement of the crystal structure of monoclinic chloritoid. Acta Crystallographica, B31, 780–784.

———(1980) The structure of triclinic chloritoid and chloritoid polymorphism. American Mineralogist, 65, 534–539.

Harrison, F.W. and Brindley, G.W. (1957) The crystal structure of chloritoid. Acta Crystallographica, 10, 77.

Hawthorne, F.C. (1981) Amphibole spectroscopy. In D.R. Veblen, Ed., Amphiboles and other hydrous Pyriboles-Mineralogy, 9A, 103–139. Reviews in Mineralogy, Mineralogical Society of America, Washington, D.C.

Helgeson, H.C., Delany, J.M., Nesbitt, H.W., and Bird, D.K. (1978): Summary and critique of the thermodynamic properties of rock-forming minerals. American Journal of Science, 278, 1–229.

Hofmeister, A.M. and Chopelas, A. (1991) Thermodynamic properties of pyrope and gossular from vibrational spectroscopy. American Mineralogist, 76, 880–897.

Hofmeister, A.M. and Mao, H.K. (2002) Redefinition of the mode Grüneisen parameter: implications for thermodynamic properties and the pressure derivative of the shear modulus. Proceedings of the National Academy of Science, 99, 559–564.

Hofmeister, A.M., Xu, J., Mao, H.-K., Bell, P.M., and Hoering T.C. (1989) Thermodynamics of Fe-Mg olivines at mantle pressures: Mid- and far-infrared spectroscopy at high pressure. American Mineralogist, 74, 281–306.

Hofmeister, A.M., Cynn, H., Burnley, P.C., and Meade C. (1999) Vibrational spectra of dense, hydrous silicates at high pressure: Importance of the hydrogen

bond angle. American Mineralogist, 84, 454–464.
Holland, T.J.B. (1989) Dependence of entropy on volume for silicate and oxide minerals: A review and a predictive model. American Mineralogist, 74, 5–13.
Holland, T.J.B. and Powell, R. (1998) An internally consistent thermodynamic data set for phases of petrological interest. Journal of Metamorphic Geology, 16, 309–343.
Ivaldi, G., Catti, M., and Ferraris, G. (1988) Crystal structure at 25 and 700°C of magnesiochloritoid from a high-pressure assemblage (Monte Rosa). American Mineralogist, 73, 358–364.
Kieffer, S.W. (1979) Thermodynamics and lattice vibrations of minerals: 3. Lattice dynamics and an approximation for minerals with application to simple substances and framework silicates. Reviews of Geophysics and Space Physics, 17, 35–39.
———(1980) Thermodynamics and lattice vibrations of minerals: 4. Application to chain and sheet silicates and orthosilicates. Reviews of Geophysics and Space Physics, 18, 862–886.
Koch-Müller, M. and Wirth, R. (2001) An experimental study of the effect of iron on magnesiochloritoid-talc-clinochlore-kyanite stability. Contributions to Mineralogy and Petrology, 141, 546–559.
Koch-Müller, M., Abs-Wurmbach, I., Langer, K., Shaw, C., Wirth, R., and Gottschalk, M. (2000a) Synthetic and natural Fe-Mg-chloritoid: structural, spectroscopic and thermodynamic studies. European Journal of Mineralogy, 12, 293–314.
Koch-Müller, M., Kahlenberg, V., Schmidt, C., and Wirth, R. (2000b) Location of OH groups and oxidation processes in triclinic chloritoid. Physics and Chemistry of Minerals, 27, 703–712.
Koch-Müller, M., Fei., Y., Hauri, E., and Liu, Z. (2001) Location and quantitative analysis of OH in coesite. Physics and Chemistry of Minerals, 28, 693–705.
Kretz, R. (1983) Symbols for rock-forming minerals. American Mineralogist, 68, 277– 279.
Levien, L. and Prewitt, C.T. (1981) High-pressure crystal structure and compressibility of coesite. American Mineralogist, 66, 324–333.
Mao, H.-K. and Hemley, R.J. (1998) New windows on the earth's deep interior. In Hemley R.J., Ed., Ultrahigh-Pressure Mineralogy, 37, 1–32. Reviews in Mineralogy, Mineralogical Society of America, Washington, D.C.
Mao, H.-K., Xu, J., and Bell, P.M. (1986) Calibration of the Ruby pressure gauge to 800 kbar under quasi-hydrostatic conditions. Journal of Geophysical Research, 91, 4673–4676.
Messiga, B., Kienast, J.R., Rebay, G., Riccardi, P., and Tribuzio, R. (1999) Cr-rich magnesiochloritoid eclogites from the Monviso ophiolites (Western Alps, Italy). Journal of Metamorphic Geology, 17, 287–299.
Moenke, H. (1962) Mineralspektren. Akademie Verlag, Berlin.
Rao, B.B. and Johannes, W. (1979) Further data on the stability of staurolite and quartz and related assemblages. Neues Jahrbuch für Mineralogie Monatshefte, 10, 437–447.
Simon, G., Chopin, C., and Schenk, V. (1997) Near-end-member magnesiochloritoid in prograde-zoned pyrope, Dora-Maira massif, western Alps. Lithos, 41, 37–57.
Theye, T. (2000) New experimental high pressure-data on chloritoid and carpholite. Berichte der Deutschen Mineralogischen Gesellschaft, Beiheft zum European Journal of Mineralogy, 12, 212.
Ulrich, H.H. and Waldbaum, D.R. (1976) Structural and other contributions to the third-law entropies of silicates. Geochimica et Cosmochimica Acta, 40, 1–24.
Vidal, O., Theye, T., and Chopin, C. (1994) Experimental study of chloritoid stability at high pressure and various f_{O2} conditions. Contribution to Mineralogy and Petrology, 118, 256–270.
Vidal, O., Goffé, B., Bousquet, R., and Parra, T. (1999) Calibration and testing of an empirical chloritoid-chlorite Mg-Fe exchange thermometer and thermodynamic data for daphnite. Journal of Metamorphic Geology, 17, 25–39.
Weidner, D.J., Sawamoto, H., Sasaki, S., and Kumazawa, M. (1984) Single crystal elastic properties of the spinel phase Mg_2SiO_4, Journal of Geophysical Research, 89, 7852–7860
Wood, B.J. (1981) Crystal field electronic effects on the thermodynamic properties of Fe^{2+} minerals. In R.C. Newton, A. Navrotsky and B.J. Wood, Eds., Thermodynamics of minerals and melts. Springer-Verlag, New York.
Zha, C.-S., Duffy, T.S., Downs, R.T., Mao, H.-K., and Hemley, R.J. (1998) Brillouin scattering and X-ray diffraction of San Carlos olivine: direct pressure determination to 32 GPa. Earth and Planetary Science Letters, 159, 25–33.

MANUSCRIPT RECEIVED JULY 31, 2001
MANUSCRIPT ACCEPTED DECEMBER 18, 2001
MANUSCRIPT HANDLED BY JAMES KUBICKI